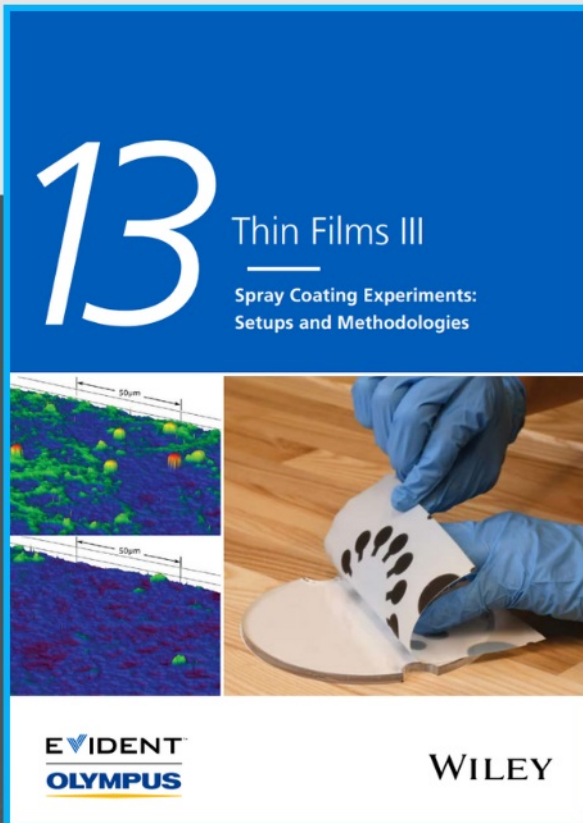




Spray Coating Experiments: Setups and Methodologies



**The latest eBook from
Advanced Optical Metrology.
Download for free.**

Spray Coating Experiments: Setups and Methodologies, is the third in our Thin Films eBook series. This publication provides an introduction to spray coating, three article digests from Wiley Online Library and the latest news about Evident's Image of the Year Award 2022.

Wiley in collaboration with Evident, are committed to bridging the gap between fundamental research and industrial applications in the field of optical metrology. We strive to do this by collecting and organizing existing information, making it more accessible and useful for researchers and practitioners alike.

EVIDENT
OLYMPUS

WILEY

Weaving Sensing Fibers into Electrochemical Fabric for Real-Time Health Monitoring

Lie Wang, Liyuan Wang, Ye Zhang, Jian Pan, Shangyu Li, Xuemei Sun, Bo Zhang, and Huisheng Peng*

Wearable sensing technologies have received considerable interests due to the promising use for real-time monitoring of health conditions. The sensing part is typically made into a thin film that guarantees high flexibility with different sensing materials as functional units at different locations. However, a thin-film sensor easily breaks during use because it cannot adapt to the soft or irregular body surfaces, and, moreover, it is not breathable or comfortable for the wearable application. Herein, a new and general strategy of making electrochemical fabric from sensing fiber units is reported. These units efficiently detect a variety of physiological signals such as glucose, Na^+ , K^+ , Ca^{2+} , and pH. The electrochemical fabric is highly flexible and maintains structural integrity and detection ability under repeated deformations, including bending and twisting. They demonstrate the capacity to monitor health conditions of human body in real time with high efficacy.

1. Introduction

Wearable sensing technologies have gained increasing interest in biomedical fields because they are convenient and could efficiently monitor health conditions by detecting various physiological signals in real time.^[1–4] Wearable sensors typically appear in a film format. The active and packing layers are sequentially deposited onto a variety of polymer substrates, resulting in a sensing film that can detect a specific physiological signal.^[5–7] In other words, one sensor can only be used for the detection of one physiological signal. After a selective coating of different active materials onto different sites of the substrate, the resulting film sensor may achieve the desirable integration and detect a variety of signal sources in one device.^[4,8–10] The integrated film sensor generally requires a complex fabrication process that has a high cost and low efficiency. To meet the requirements for wearable electronics, the film sensor has typically been made as thin as

possible, making it fragile and, thus, difficult to work with during the fabrication process and prone to breaking during body deformation.^[11,12] It remains a challenge for thin-film sensors to effectively adapt to the irregular and soft surface of our bodies. Moreover, they are neither breathable nor comfortable, whereas comfort and breathability are highly desired for wearable electronics.^[13] The above difficulties have largely limited the further development of wearable sensors and thus the advancement of related applications in a spectrum of fields alongside the biomedical facilities.^[14–16]

The ancient textile technology may provide an inspiration to simultaneously solve the above problems.^[17–19] If different sensing materials that respond to different environmental stimuli are coated onto fiber substrates,

the resulting fiber sensors can then be woven into a fabric that could detect a variety of physiological signals. Compared with the traditional thin-film sensor, the fabric sensor can bear various complex, even severe deformations such as twisting, while provides an effective and comfortable interface with human skin (i.e., the fabric is breathable and comfortable). Thus, the fabric sensor would allow for a long-term use without discomfort for the users and can be manufactured on a large scale for practical applications. However, to our best knowledge, such an integrated fabric sensor is currently unavailable.

Here, we demonstrate the realization of the integrated electrochemical fabric as a promising wearable platform for real-time health monitoring by weaving different kinds of sensing fibers as the building blocks. The sensing fibers are constructed by coating active materials onto carbon nanotube (CNT) fibers to form a coaxial structure. Several representative physiological signals (e.g., glucose, Na^+ , K^+ , Ca^{2+} , and pH) were tested to demonstrate the effectiveness of the novel fabric sensor. The resulting integrated fabric maintained a high real-time sensing performance under repeated deformations, including both bending and twisting.

2. Results and Discussion

2.1. Preparation of Multifunctional Fibers

Figure 1 schematically illustrates the fabrication processes of the sensing fiber and the resulting electrochemical fabric.

L. Wang, L. Wang, Dr. Y. Zhang, J. Pan, S. Li, Dr. X. Sun, Dr. B. Zhang, Prof. H. Peng
State Key Laboratory of Molecular Engineering of Polymers
Department of Macromolecular Science and Laboratory of Advanced Materials
Fudan University
Shanghai 200438, China
E-mail: penghs@fudan.edu.cn

 The ORCID identification number(s) for the author(s) of this article can be found under <https://doi.org/10.1002/adfm.201804456>.

DOI: 10.1002/adfm.201804456

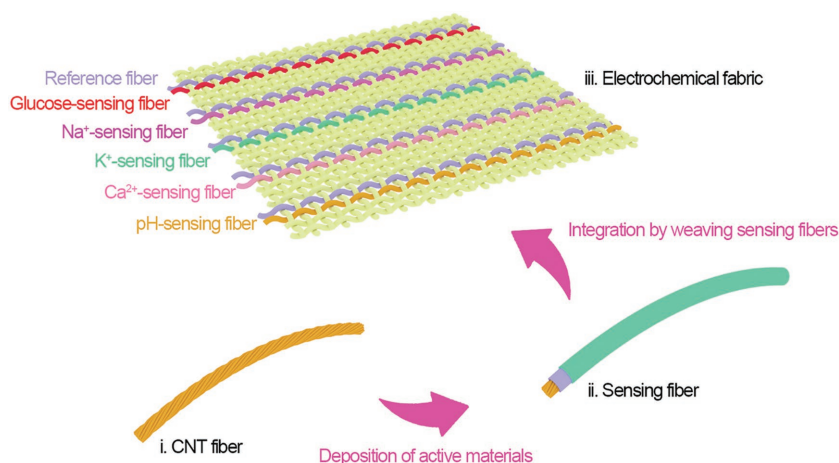


Figure 1. Schematic illustration for the fabrication of the electrochemical fabric by weaving sensing fibers, that are made by depositing active materials on carbon nanotube (CNT) fiber substrates.

Different kinds of sensing fibers were first fabricated by depositing active materials onto CNT fiber electrodes (Figure S1, Supporting Information). For example, the glucose-sensing fiber was constructed by electrodepositing Prussian blue (PB) as a mediator to provide better sensitivity, while glucose oxidase, immobilized within a permeable film of the chitosan, was coated as the active layer (Figure S2, Supporting Information). The ion-sensing fibers were obtained with especially ion-selective ionophore and poly(3,4-ethylenedioxythiophene):poly(styrene sulfonate) (PEDOT:PSS) as an ion-to-electron transducer due to its large impedance change to ion concentration (Figure S3, Supporting Information). The pH-sensing fiber was made by electrodepositing polyaniline (PANI) onto the CNT fiber, which shows larger zeta potential changes at different pH values due to the PANI surface protonation changes at different pH values (Figure S4, Supporting Information). These different kinds of sensing fibers were woven into an integrated electrochemical fabric. Note that, for each sensing functionality, a sensing fiber served as the work electrode while a Ag/AgCl fiber was used as the reference electrode (Figure S5, Supporting Information).

2.2. Characterization of the Prepared Fibers

The CNT fiber electrodes played a crucial role in the high sensing performances of the sensing fibers due to the combined high electronic, electrochemical, and mechanical properties.^[20,21] For instance, they exhibited electrical conductivities of 10^2 – 10^3 S cm⁻¹ and tensile strengths of 10^2 – 10^3 MPa.^[22] They were flexible with the electrical resistance being maintained after bending for 1000 cycles (Figure 2a), which exceeded the other commonly used conductive fibers such as carbon fiber and Au wire. Cyclic voltammograms (CV) in Figure 2b for Fe(CN)₆^{3-/4-} redox coupling also indicated the higher charge storage capacity of the CNT fiber over the carbon fiber and Au wire. The normalized area (effective electrochemically active surface area/geometric surface area) of fiber electrodes was estimated by using the Randles–Sevcik equation from the CV

curves.^[23,24] The CNT fiber electrode showed a normalized area of 1.82, which was 15 times that of the carbon fiber and 33 times that of the Au wire (Figure 2c). This was because the building of CNTs in the fiber formed nanoscale voids and enhanced electrochemically active surface areas (Figure 2d,e). Therefore, the CNT fiber electrodes were favorable for the electrodeposition of functional materials, aiming for a high-performance sensing fibers (Figures S6 and S7, Supporting Information).

Figure 2f presents a typical scanning electron microscopy (SEM) image of the PB layer of a glucose-sensing fiber. Both PB and glucose oxidase active layers had been uniformly produced on the CNT fiber (Figure 2g), so were the other sensing fibers and the Ag/AgCl reference fiber (Figures S8–S10, Supporting Information).

Based on the all-solution process, the sensing fibers can be continuously produced on a large scale (e.g., Figure 2h shows a roll of glucose-sensing fiber). The sensing fibers were highly flexible and maintained the structure and property stability under various deformations (Figure 2i,j), making it favorable for wearable applications.

2.3. In Vitro Performance of the Prepared Fibers

The performances of the sensing fibers were then monitored separately with different analyte solutions, and a two-electrode system with a Ag/AgCl fiber reference electrode was used as the research model. Compared with the commercial solid-state Ag/AgCl electrode, the designed Ag/AgCl fiber electrode here showed a smaller potential difference in the presence of different chloride ion concentrations (Figure 3a). The potential was also well maintained in the presence of different anionic and cationic solutions (Figure S11, Supporting Information). The stability of the designed Ag/AgCl fiber electrode was attributed to the polyvinyl butyral (PVB) layer, which contained saturated NaCl for the stable potential, regardless of the ionic strengths of the solutions.^[25]

The glucose-sensing fibers worked effectively at the linear range of 0– 200×10^{-6} M with a sensitivity of 2.15 nA μM⁻¹ (Figure 3b). These glucose concentrations cover the typical sweat glucose concentrations of normal people.^[26,27] Figure 3c–e shows the open-circuit potentials of Na⁺, K⁺, and Ca²⁺-sensing fibers in the electrolyte solutions with physiologically relevant concentrations of $(10$ – $160) \times 10^{-3}$ M Na⁺, $(2$ – $32) \times 10^{-3}$ M K⁺, and $(0.5$ – $2.53) \times 10^{-3}$ M Ca²⁺. Excellent sensing performances were found for Na⁺, K⁺, and Ca²⁺-sensing fibers with sensitivities of 45.8, 35.9, and 52.3 mV dec⁻¹ of concentration, respectively. Figure 3f illustrates the general performance of a pH-sensing fiber in solutions with pH values from 4 to 7. There also showed a linear relationship between open-circuit potential and pH. The reproducibility of the sensing fiber was verified with insignificant fluctuations (Figure 4).

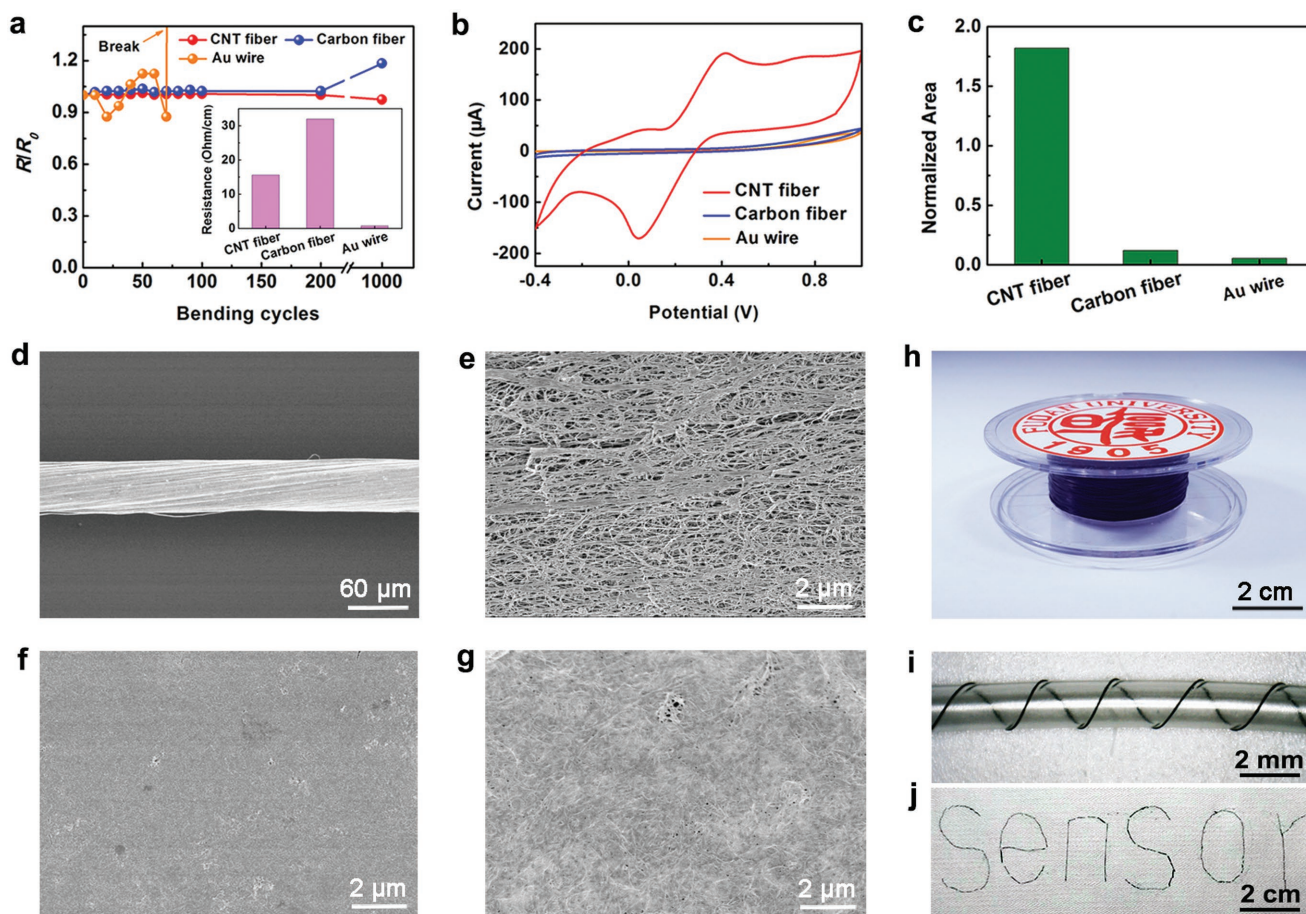


Figure 2. Characterization of the sensing fibers. a) Dependence of electrical resistance on the fiber electrode from bending cycle number at a bending angle of 90° . Here R_0 and R correspond to the electrical resistances before and after bending. The inset shows the initial electrical resistances of fiber electrodes. b) CV plots of the different fiber electrodes in phosphate-buffered saline (PBS) with $\text{Fe}(\text{CN})_6^{3-/4-}$ (scan rate of 100 mV s^{-1} with a commercial Ag/AgCl electrode). c) Normalized areas of the different fiber electrodes. SEM images of the CNT fiber at d) low and e) high magnifications. SEM images of the f) PB and g) glucose oxidase layers of the glucose-sensing fiber. h) Photograph of a roll of glucose-sensing fiber. Photographs of a glucose-sensing fiber i) wrapped around a tube and j) woven into a fabric with the letters of “sensor.”

The selectivity of a wearable electrochemical sensor is crucial, because various metabolites in sweat can influence the performance of the sensor. In this study, interfering ions were intentionally added to the target electrolyte solution. The change in current or potential due to addition of such ions was recorded and found to be significantly smaller than the response for the target ion (Figure 5). Therefore, these sensing fibers displayed a high selectivity. The long-term performance of these sensing fibers was further confirmed in Figure S12 (Supporting Information).

We then wove the above sensing fibers into a fabric. Figure 6a shows an SEM image of a set of glucose sensors in which the glucose-sensing fiber and Ag/AgCl fiber were tightly woven into the fabric. It should be noted that a fabric consists of thousands of fibers; therefore, many different kinds of sensing fibers can be integrated. Herein, as an application demonstration, five kinds of sensing fibers (i.e., those responding to glucose, Na^+ , K^+ , Ca^{2+} , and pH) were made into an electrochemical fabric to monitor sweat metabolites. Figure 6b shows a $4.5 \text{ cm} \times 6 \text{ cm}$ electrochemical fabric that could easily absorb the simulated sweat. The fabric could bear a lot of bending and

twisting cycles without obvious fatigue in sensing performance (Figure 6c,d). Moreover, it also possesses good level of washing and rubbing durability (Figure S13, Supporting Information). Furthermore, the system-level interference studies of the electrochemical fabric indicated that the sensing fibers maintained the high selectivity upon varying concentrations of each analyte (Figure 6e).

2.4. In Situ Performance of the Prepared Fibers

For the in situ analysis of the sweat, the electrochemical fabric was further made into a garment (Figure S14, Supporting Information) and connected to two flexible integrated chips (Figure S15, Supporting Information), which in turn wirelessly transferred data to a Bluetooth-enabled smartphone, with a custom-developed application downloaded (Figures S16 and S17, Supporting Information). Interestingly, a flexible fiber-shaped lithium-ion battery could be effectively woven into the garment as the power supply (Figure S18, Supporting Information).^[28,29] As shown in Figure 7a, a subject is dressed

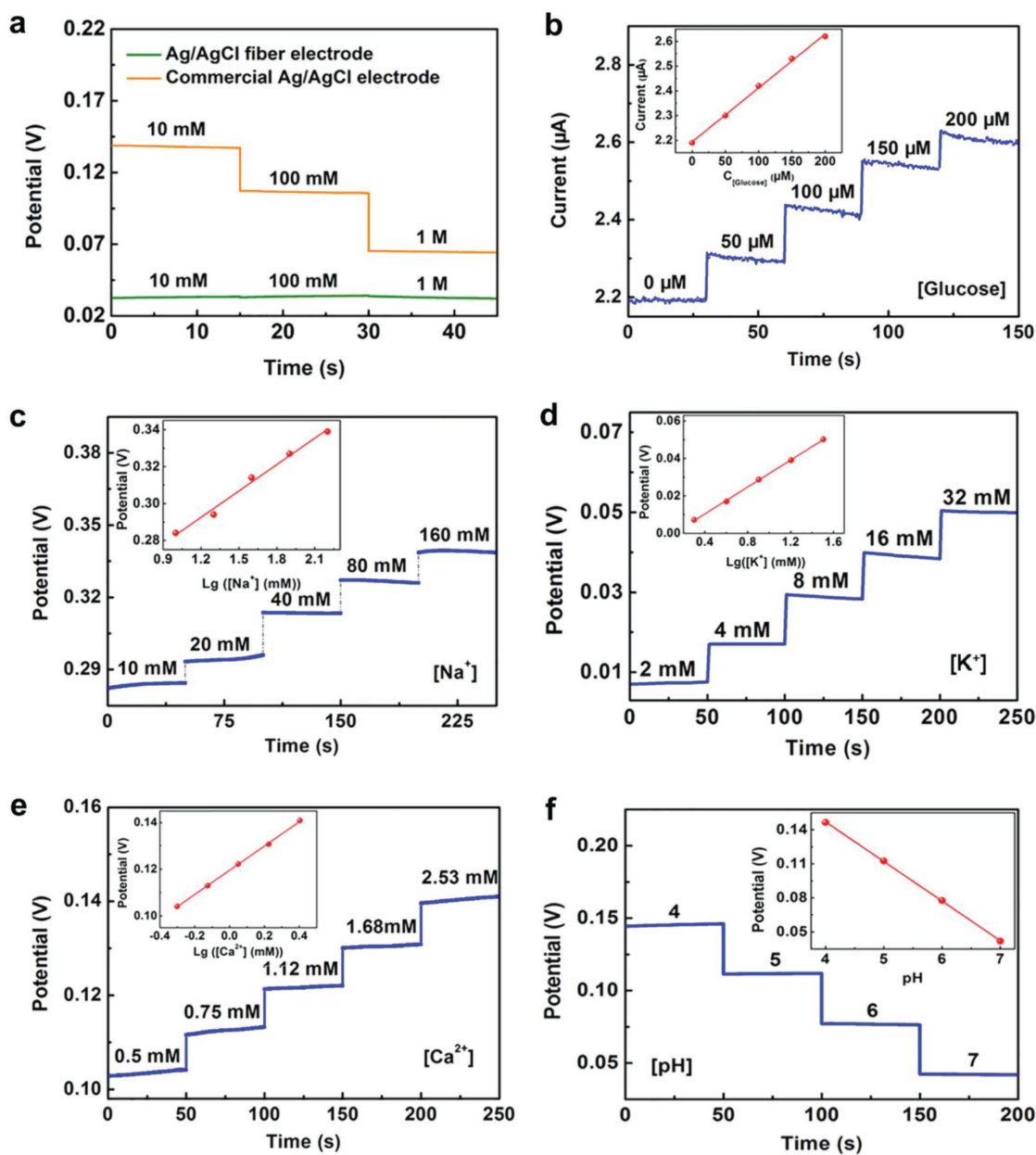


Figure 3. a) Potential stability of the as-synthesized Ag/AgCl fiber electrode as compared to a commercial solid-state Ag/AgCl electrode. b) The chronoamperometric response of the glucose-sensing fiber to the respective analyte solutions in phosphate-buffered saline (PBS). c–f) The open-circuit potential responses of the Na^+ , K^+ , Ca^{2+} , and pH-sensing fibers to the respective analyte solutions in PBS.

the garment and running. After ≈ 10 min, the sweat permeated into the fabric, and a real-time analysis showed that the signals could be stably obtained (Figure 7b). The accuracy of in situ analysis was further verified by comparing the on-body sensor readings with ex situ measurements from collected sweat samples following the same running exercise for 35 min (Figure 7c).

3. Conclusions

In conclusion, we have developed a wearable electrochemical fabric by integrating different kinds of sensing fibers as a

powerful platform for real-time health monitoring. Five physiological signals, i.e., glucose, Na^+ , K^+ , Ca^{2+} , and pH, were simultaneously acquired by the fabric, and the sensing performance can be well maintained under repeated deformations (such as bending and twisting). This work provides a general and promising strategy in the development of the next-generation wearable sensors and the other flexible electronic devices. To our best knowledge, this is the first report of an integrated electrochemical fabric sensor that can efficiently detect a variety of physiological signals, representing an important step toward practical applications. This report opens up a new direction for wearable sensors, which may be commercialized for diversified

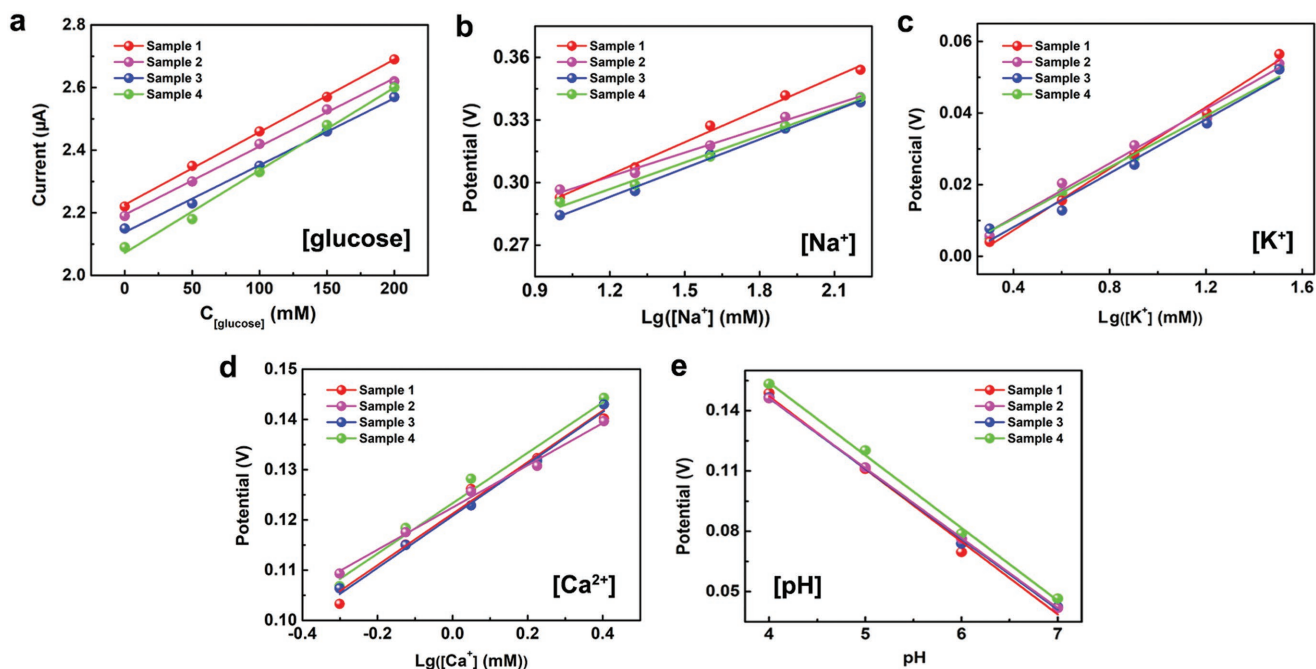


Figure 4. The reproducibility of a) glucose, b) Na^+ , c) K^+ , d) Ca^{2+} , and e) pH-sensing fibers. The four colors represent four different samples for each kind of sensor.

applications in the near future. On the other hand, it still needs to be further improved for practical applications in the future. For example, the glucose oxidase cannot be used for a long time, which could be optimized by using nonenzymatic active material.^[30,31] Besides, the safety issue of using CNTs should be cautious,^[32,33] and here the CNTs with lengths of up to millimeters cannot be swallowed by cells for high safety, which may be further enhanced by sealing the sensing fiber carefully.

4. Experimental Section

Materials: Glucose oxidase (G109029-10KU), single-walled carbon nanotube (SWCNT, C140995), valinomycin (potassium ionophore) (V100895), bis(2-ethylehexyl) sebacate (DOS) (G105169), tetrahydrofuran (T120775), PVB resin BUTVAR B-98 (G105915), and multiwalled carbon nanotube (MWCNT, C121257) were purchased from Aladdin Reagent. Sodium ionophore X (#71747), calcium ionophore II (#21193), sodium tetraphenylborate (NaTPB, #72018), sodium

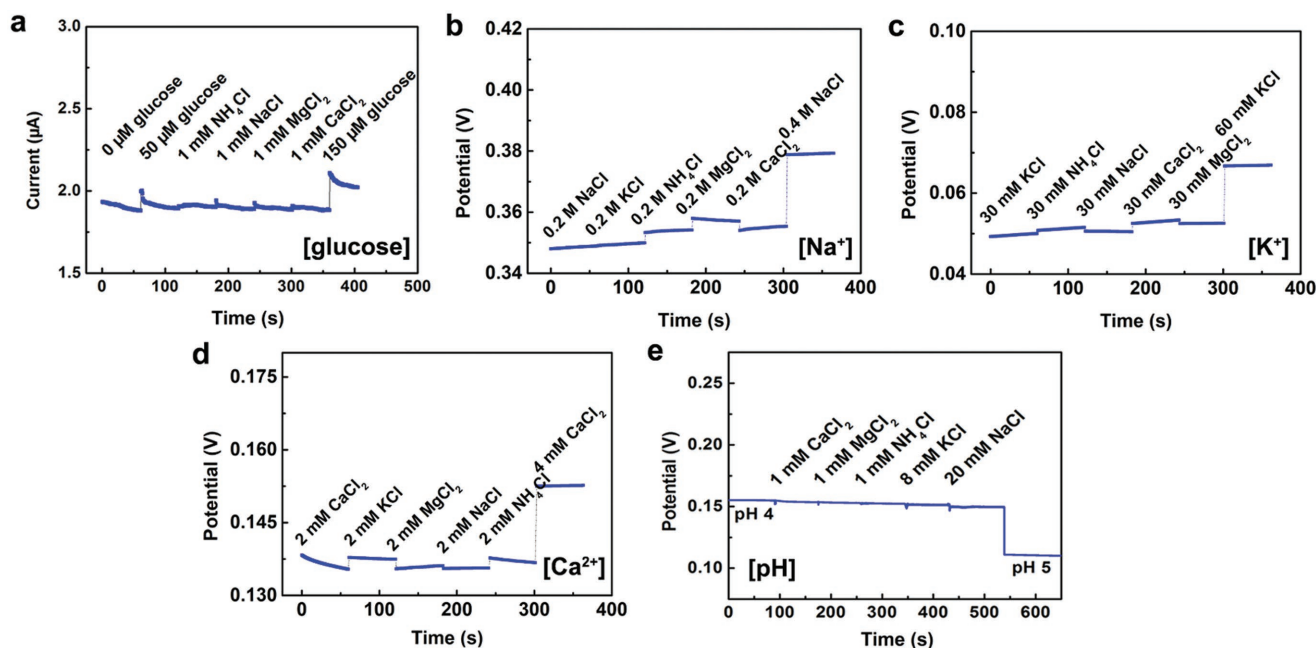


Figure 5. The interference study for individual a) glucose, b) Na^+ , c) K^+ , d) Ca^{2+} , and e) pH-sensing fibers.

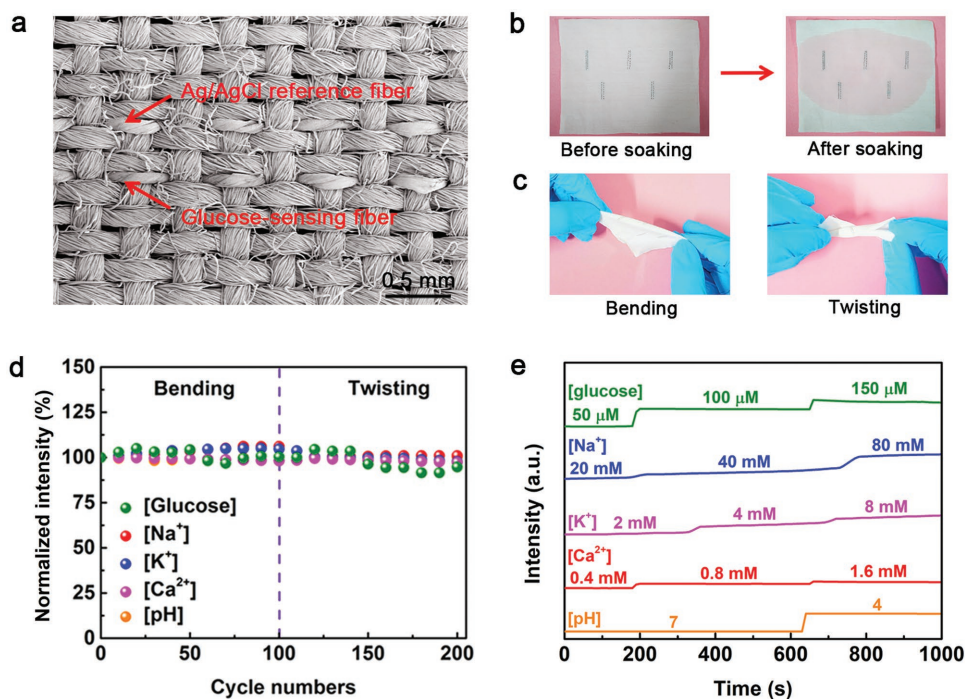


Figure 6. Performance and characterization of the electrochemical fabric through the integration of different kinds of sensing fibers. a) SEM image of glucose-sensing and Ag/AgCl reference fibers in the fabric. b) Photograph of a 4.5 cm × 6 cm electrochemical fabric before and after soaking (with simulated sweat). c) Photograph of a 4.5 cm × 6 cm electrochemical fabric under bending and twisting. d) Flexibility of the sensing fibers in electrochemical fabric under repeated bending and twisting. e) System-level interference studies of the sensing fibers in electrochemical fabric.

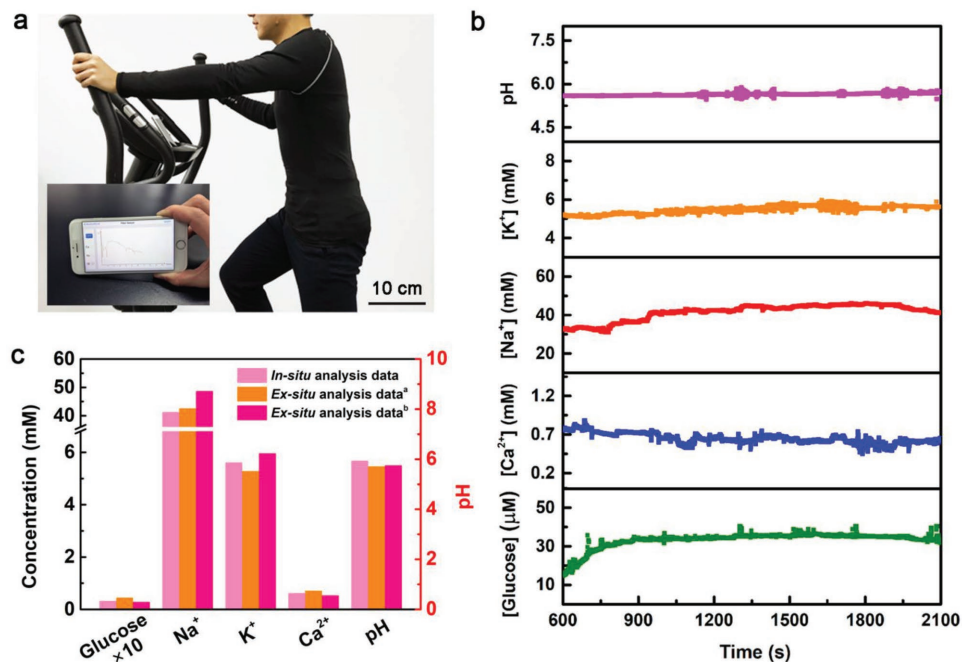


Figure 7. Application and demonstration of the integrated electrochemical fabric. a) Photograph of a subject wearing the garment device while running. The inset shows a smartphone that wirelessly receives data with a custom-developed application. b) Real-time sweat analysis using the garment device. c) Comparison of ex situ data from the collected sweat samples with that of the in situ. ^a Measured by using sensing fibers. ^b Measured by using ICP-AES (Na⁺, K⁺, and Ca²⁺), pH meter (pH), and the enzyme-electrode method (glucose).

tetrakis[3,5-bis(trifluoromethyl)phenyl] borate (Na-TFPB, #72017), block polymer poly(ethylene oxide)–poly(propylene oxide)–poly(ethylene oxide) (PEO–PPO–PEO) (F127, #P2443), high-molecular-weight polyvinyl chloride (PVC, #81387), 3,4-ethylenedioxythiophene (EDOT, #483028) and poly(sodium 4-styrenesulfonate) (NaPSS, #243051) were obtained from Sigma Aldrich. Phosphate-buffered saline (PBS) was acquired from Solarbio Science and Technology Co., Ltd. All other common reagents were purchased from Sinopharm Chemical Reagent Co., Ltd.

Synthesis of Carbon Nanotube Fibers: CNT fibers were synthesized via floating catalyst vapor deposition with ferrocene and thiophene as catalysts, flowing hydrogen (1600 sccm) as reducing gas, and argon (200 sccm) as carrier gas at 1200 °C.^[34]

Preparation of the Ag/AgCl Fiber Electrode: A layer of Ag was first electrodeposited onto the CNT fiber in a 5×10^{-3} M AgNO₃/1 M KNO₃ solution by cyclic voltammetry from –0.9 to 0.9 V for 14 cycles at 100 mV s⁻¹. Chlorination was then carried out in a 0.1 M HCl/0.01 M KCl solution by cyclic voltammetry from –0.15 to 1.05 V for four cycles at 50 mV s⁻¹. To minimize the potential drift, a layer of PVB solution was coated onto the fiber electrode. The PVB solution was prepared by dissolving 79.1 mg PVB, 50 mg NaCl, 2 mg F127, and 0.2 mg MWCNT into 1 mL methanol.

Preparation of Glucose-Sensing Fibers: Chitosan was first dissolved in acetic acid under magnetic stirring to form a 1 wt% chitosan solution. The chitosan solution was then mixed with SWCNT (2 mg mL⁻¹) and glucose oxidase (40 mg mL⁻¹) under ultrasonic treatment for 30 min, forming a viscous mixed solution. In order to improve the sensitivity of the glucose-sensing fiber, a thinner PB mediator layer was electrochemically deposited onto the CNT fibers in a 2.5×10^{-3} M FeCl₃, 100×10^{-3} M KCl, 2.5×10^{-3} M K₃Fe(CN)₆, and 100×10^{-3} M HCl mixture solution. Then, 4 μL of chitosan/SWCNT/glucose oxidase mixed solution was drop-coated onto the CNT/PB electrode to obtain the glucose-sensing fiber.

Preparation of Na⁺, K⁺, Ca²⁺, and pH-Sensing Fibers: The Na⁺ selective membrane precursor was prepared by dissolving 100 mg of a mixture containing Na-TFPB, high-molecular-weight PVC, DOS, and sodium ionophore X (weight ratios of 0.55/33/65.45/1) in 660 μL tetrahydrofuran. The K⁺-selective membrane precursor was prepared by dissolving 100 mg of a mixture containing NaTPB, PVC, DOS, and potassium ionophore (weight ratios of 0.5/32.75/64.75/2) in 350 μL cyclohexanone. The Ca²⁺-selective membrane precursor was prepared by dissolving 100 mg of a mixture containing Na-TFPB, PVC, DOS, and calcium ionophore II (weight ratios of 0.55/33/65.45/1) in 660 μL tetrahydrofuran. The ion-selective membrane precursor solutions were sealed and stored at 4 °C. PEDOT:PSS was deposited onto the CNT fiber by galvanostatic electrochemical polymerization with an external Ag/AgCl reference electrode from a solution containing 0.01 M EDOT and 0.1 M NaPSS. Ion-selective membranes were then prepared by drop-casting the ion-selective membrane precursor solutions onto their corresponding electrodes. In the case of the pH-sensing fiber, PANI was electrodeposited onto the CNT fiber in a 0.1 M aniline/0.1 M H₂SO₄ solution by cyclic voltammetry from –0.2 to 1 V for 25 cycles at 100 mV s⁻¹.

Characterization of the Sensing Fibers: The glucose-sensing fibers were characterized from the respective analyte solutions in PBS by using amperometric *I*–*t* curve at 0.42 V (vs Ag/AgCl reference electrode). The Na⁺, K⁺, Ca²⁺, and pH-sensing fibers were characterized in their respective analyte solutions by using real-time open-circuit potential measurements. All the electrochemical measurements were conducted using a CHI666e electrochemical workstation. The structures of the fiber electrodes and sensing fibers were characterized by SEM (Hitachi, FE-SEM S-4800 operated at 1 kV). The washability of the electrochemical fabric was tested by a commercial washing machine (XPB20-32, CHIGO), and the whole washing process lasted for 10 min. The rubbing resistance of the electrochemical fabric was tested by rubbing it on a cotton cloth with stress of ≈1 N.

Analysis of Sweat: The experiment protocols were approved by Animal and Human Experimentation Committee of Fudan University. A healthy male subject was recruited from the Fudan University and gave written, informed consent before participating in the study. The sensing fibers

were woven into a fabric and further made into a garment. A flexible integrated chip was used to wirelessly transfer data to a Bluetooth-enabled smartphone. For in situ analysis, the subject wore the garment device under running conditions. The sensing data were directly recorded on the smartphone via a customized application. The sweat was simultaneously collected after running for 35 min to compare in situ data with ex situ data. For ex situ analysis, glucose of the sample was measured by the enzyme-electrode method according to GB/T 16285-2008 criterion and glucose-sensing fiber. Na⁺, K⁺, and Ca²⁺ of the sample were measured by inductively coupled plasma-atomic emission spectrometry (ICP-AES) (iCAP 7400, Thermo Scientific) and ion-sensing fibers. pH of the sample was measured by a pH meter (PHS 3C, INESA) and pH-sensing fiber.

Fabrication of Fiber-Shaped Lithium-Ion Batteries: LiCoO₂ and graphite were first coated on stainless steel wire and Cu wire as anode and cathode, respectively. The composite-yarn anode and cathode were then inserted into a heat-shrinkable tube with a separator between them. Finally, the electrolyte LB303 was injected into the tube in an argon-filled glove box to obtain the fiber-shaped lithium-ion batteries.

Supporting Information

Supporting Information is available from the Wiley Online Library or from the author.

Acknowledgements

L.W. and L.W. contributed equally to this work. This work was supported by the Ministry of Science and Technology of China (2016YFA0203302), National Natural Science Foundation of China (Grants Nos. 21634003, 51573027, 51403038, 51673043, and 21604012), and the Science and Technology Commission of Shanghai Municipality (Grant Nos. 16JC1400702, 15XD1500400, and 15JC1490200). The authors are grateful to Austin Barrett and Dr. Wei Tao from Harvard Medical School for their language editing.

Conflict of Interest

The authors declare no conflict of interest.

Keywords

carbon nanotubes, electrochemical fabrics, fibers, real-time health monitoring, sensors

Received: June 29, 2018

Revised: July 27, 2018

Published online: September 4, 2018

- [1] J. Zhou, X. Xu, Y. Xin, G. Lubineau, *Adv. Funct. Mater.* **2018**, *28*, 1705591.
- [2] A. Tricoli, N. Nasiri, S. De, *Adv. Funct. Mater.* **2017**, *27*, 1605271.
- [3] W. Liu, M. Liu, R. Ma, R. Zhang, W. Zhang, D. Yu, Q. Wang, J. Wang, H. Wang, *Adv. Funct. Mater.* **2018**, *28*, 1705928.
- [4] W. Gao, S. Emaminejad, H. Y. Y. Nyein, S. Challa, K. Chen, A. Peck, H. M. Fahad, H. Ota, H. Shiraki, D. Kiriya, D. Lien, G. A. Brooks, R. W. Davis, A. Javey, *Nature* **2016**, *529*, 509.
- [5] H. Kudo, T. Sawada, E. Kazawa, H. Yoshida, Y. Iwasaki, K. Mitsubayashi, *Biosens. Bioelectron.* **2006**, *22*, 558.

- [6] T. Guinovart, G. Valdés-Ramírez, J. R. Windmiller, F. J. Andrade, J. Wang, *Electroanalysis* **2014**, *26*, 1345.
- [7] J. Kim, R. Kumar, A. J. Bandothkar, J. Wang, *Adv. Electron. Mater.* **2017**, *3*, 1600260.
- [8] S. Imani, A. J. Bandothkar, A. M. V. Mohan, R. Kumar, S. Yu, J. Wang, P. P. Mercier, *Nat. Commun.* **2016**, *7*, 11650.
- [9] H. Lee, T. K. Choi, Y. B. Lee, H. R. Cho, R. Ghaffari, L. Wang, H. J. Choi, T. D. Chung, N. Lu, T. Hyeon, S. H. Choi, D. H. Kim, *Nat. Nanotechnol.* **2016**, *11*, 566.
- [10] H. Y. Y. Nyein, W. Gao, Z. Shahpar, S. Emaminejad, S. Challa, K. Chen, H. M. Fahad, L. Tai, H. Ota, R. W. Davis, A. Javey, *ACS Nano* **2016**, *10*, 7216.
- [11] X. Xuan, H. S. Yoon, J. Y. Park, *Biosens. Bioelectron.* **2018**, *109*, 75.
- [12] Y. S. Rim, S. Bae, H. Chen, N. D. Marco, Y. Yang, *Adv. Mater.* **2016**, *28*, 4415.
- [13] W. Weng, P. Chen, S. He, X. Sun, H. Peng, *Angew. Chem., Int. Ed.* **2016**, *55*, 6140.
- [14] J. Kim, H. J. Shim, J. Yang, M. K. Choi, D. C. Kim, J. Kim, T. Hyeon, D. H. Kim, *Adv. Mater.* **2017**, *29*, 1700217.
- [15] J. Rivnay, S. Inal, A. Salleo, R. M. Owens, M. Berggren, G. G. Malliaras, *Nat. Rev. Mater.* **2018**, *3*, 17086.
- [16] L. Tai, W. Gao, M. Chao, M. Bariya, Q. P. Ngo, Z. Shahpar, H. Y. Y. Nyein, H. Park, J. Sun, Y. Jung, E. Wu, H. M. Fahad, D. Lien, H. Ota, G. Cho, A. Javey, *Adv. Mater.* **2018**, *30*, 1707442.
- [17] R. F. Service, *Science* **2003**, *301*, 909.
- [18] W. Zeng, L. Shu, Q. Li, S. Chen, F. Wang, X. M. Tao, *Adv. Mater.* **2014**, *26*, 5310.
- [19] J. Ren, Y. Zhang, W. Bai, X. Chen, Z. Zhang, X. Fang, W. Weng, Y. Wang, H. Peng, *Angew. Chem., Int. Ed.* **2014**, *53*, 7864.
- [20] P. Chen, Y. Xu, S. He, X. Sun, S. Pan, J. Deng, D. Chen, H. Peng, *Nat. Nanotechnol.* **2015**, *10*, 1077.
- [21] P. Xu, B. Wei, Z. Cao, J. Zheng, K. Gong, F. Li, J. Yu, Q. Li, W. Lu, J. H. Byun, B. S. Kim, Y. Yan, T. W. Chou, *ACS Nano* **2015**, *9*, 6088.
- [22] J. N. Wang, X. G. Luo, T. Wu, Y. Chen, *Nat. Commun.* **2014**, *5*, 3848.
- [23] S. Hrapovic, Y. Liu, K. B. Male, J. H. T. Luong, *Anal. Chem.* **2004**, *76*, 1083.
- [24] S. J. Konopka, B. McDuffie, *Anal. Chem.* **1970**, *42*, 1741.
- [25] T. Guinovart, G. A. Crespo, F. X. Rius, F. J. A. Andrade, *Anal. Chim. Acta* **2014**, *821*, 72.
- [26] J. Moyer, D. Wilson, I. Finkelshtein, B. Wong, R. Potts, *Diabetes Technol. Ther.* **2012**, *14*, 398.
- [27] O. Olarte, J. Chilo, J. Pelegri-Sebastian, K. Barbé, W. V. G. Moer, *Conf. Proc. IEEE Eng. Med. Biol. Soc.* **2013**, *2013*, 1462.
- [28] Y. Zhang, Y. Zhao, J. Ren, W. Weng, H. Peng, *Adv. Mater.* **2016**, *28*, 4524.
- [29] Y. Zhang, W. Bai, X. Cheng, J. Ren, W. Weng, P. Chen, X. Fnag, Z. Zhang, H. Peng, *Angew. Chem., Int. Ed.* **2014**, *53*, 14564.
- [30] H. Li, C. Y. Guo, C. L. Xu, *Biosens. Bioelectron.* **2015**, *63*, 339.
- [31] R. Ahmad, M. S. Ahn, Y. B. Hahn, *Electrochem. Commun.* **2017**, *77*, 107.
- [32] K. Donaldson, R. Aitken, L. Tran, V. Stone, R. Duffin, G. Forrest, A. Alexander, *Toxicol. Sci.* **2006**, *92*, 5.
- [33] E. A. Iyiegbuniwe, U. U. Nwosu, S. Kodali, *Int. J. Environ. Sci. Dev.* **2016**, *7*, 849.
- [34] P. Liu, Y. Li, Y. Xu, L. Bao, L. Wang, J. Pan, Z. Zhang, X. Sun, H. Peng, *Small* **2018**, *14*, 1702926.